

Nucleation and Growth of Nanoscale to Microscale Cylindrical Pits in Highly-ordered Pyrolytic Graphite upon Hyperthermal Atomic Oxygen Exposure

KENNETH T. NICHOLSON
S. J. SIBENER¹

The James Franck Institute and Department of Chemistry, The University of Chicago, 5640 South Ellis Avenue, Chicago, IL 60637, USA

TIMOTHY K. MINTON¹

Department of Chemistry and Biochemistry, 108 Gaines Hall, Montana State University, Bozeman, MT 59717, USA

(Received 30 September 2003; accepted 15 January 2004)

Abstract: The erosion of highly-ordered pyrolytic graphite (HOPG) caused by exposure to hyperthermal atomic O(³P) atoms was explored. Profilometry has revealed that the overall erosion yield is linear with respect to increasing atomic oxygen exposure at a constant sample temperature of 373 K. Atomic force microscopy (AFM) was employed to image the eroded material that contains numerous nanoscale to microscale cylindrical etch pits. As there is also a linear relationship between the etch pit diameter and atomic oxygen fluence, it is proposed that the largest cylinders are nucleated at or near the topmost sheet of the original graphite material. There is a large distribution of depths for cylinders of a chosen diameter. This suggests that the chemical and physical nature of the nucleation event plays a key role in the final depth of the etch pit.

Key Words: Graphite, atomic oxygen, atomic force microscopy (AFM)

1. INTRODUCTION

Carbon-based materials, such as organic thin films, polymers, and carbon-fibre-reinforced composites, are commonly utilized on spacecraft because of their low weight and desirable chemical and mechanical properties. In the low-Earth orbital environment, hyperthermal collisions between O(³P) atoms and spacecraft, either alone or in combination with vacuum ultraviolet (VUV) light and charged particles, frequently produce chemical and physical changes in these materials that result in erosion and degradation [1]. Atomic oxygen dominates the rarefied atmosphere at ~200 to ~700 km where, a combination of impact velocity and O-atom density yields a fluence of approximately 10¹⁵ O atoms

$\text{cm}^{-2} \text{s}^{-1}$ on the ram surfaces of spacecraft. The relative velocity between the spacecraft and ambient O atoms leads to collisions that are equivalent to O atoms with mean collision energy of ~ 4.5 eV striking the ram surfaces [2].

A predictive understanding of the fundamental chemical reactivity and dynamics behind hyperthermal (0.1–20 eV) collisions of gaseous species with organic surfaces is needed in order to assess the long-term behaviour of current materials in LEO and to design more durable materials for use on future spacecraft. Highly-ordered pyrolytic graphite (HOPG) is a useful model surface to begin this kind of investigation. HOPG has a well-defined structure and may be simply described as a collection of compressed sheets of basal-plane carbon [3].

The reactivity of HOPG with O_2 and/or air has been investigated by several research groups [4]. Pristine and defected HOPG are nearly unreactive to O_2 at room temperature. Upon heating the sample to temperatures greater than 775 K, O_2 reacts only at the defect sites to create single and multilayer erosion pits with diameters on the order of 1–200 nm [5]. Using an Ar^+ or Cs^+ ion beam, defect arrays may be intentionally created [6] that can be used as templates for micro- and nanostructure design [7].

The chemical reactivity of HOPG in LEO is apparently much higher than in an O_2 environment. Ngo and coworkers have reported images of a highly eroded graphite surface after exposure to a low-Earth orbit chemical environment for an estimated fluence of 2.3×10^{20} atoms cm^{-2} [8]. Several ‘hillocks’ of varying size and shape have been observed with an average RMS roughness for a $7 \mu\text{m} \times 7 \mu\text{m}$ area of ~ 85 nm. Approximately one C atom was etched for every eight impinging O atoms (or 1.1×10^{-24} cm^3 O atom $^{-1}$). This is roughly equivalent to one atomic layer for every 10 s in LEO at an altitude of ~ 300 km. The temperature of the samples was assumed to be near 300 K, although the actual temperature of the samples was never directly measured.

Graphite erosion at these high kinetic rates appears to be directly related to both the hyperthermal translational energy (5 eV) and the high flux of atomic oxygen impinging upon the surface. We have undertaken a series of experiments to further explore the complex chemical reactivity of hyperthermal atomic O(3P) with HOPG at rates commensurate with those believed to exist in LEO. In a previous communication, the temperature dependence of this dynamic chemistry has been reported [9]. In summary, the erosion rate triples upon increasing sample temperature from 300 to 493 K during atomic oxygen exposure. Furthermore, the surface morphology changes dramatically. Cylindrical pits, spanning the nanometer to micrometer length scales, have been observed in the eroded areas when the sample is exposed at 300 K. A very rough, matted surface has been imaged for exposures at 493 K, similar to what was reported for the erosion of graphite in LEO.

There appear to be several key factors that play a role in the chemistry of energetic O(3P) with HOPG. First, the reactivity of a pristine graphite layer must be considered. Specifically, it is the rate at which a carbon atom (k_{basal}) is removed from an atomically perfect graphite sheet that leads to the formation of a point defect. The carbon atoms surrounding the defect site (k_{prism}) may be more reactive to hyperthermal atomic oxygen and therefore have a higher reaction rate constant. These reaction rates, both of which may be temperature dependent, lead to the erosion of perfect HOPG. However, no material is

perfect and many kinds of defects exist in the unreacted graphite with specific physical and chemical characteristics. These original defects may include point sites that extend for only one atomic layer. Line defects, dislocation boundaries, and grain boundaries could penetrate more deeply, spanning many atomic layers into the material. All of these classes of defects may also be buried deep within the HOPG as well, not even involved in the surface chemistry until exposed during the erosion process. The role of these imperfections is paramount to understanding the overall erosion chemistry of HOPG at a fundamental level.

This article describes the nucleation and growth of large cylindrical etch-pits observed in the eroded area of HOPG after exposure to hyperthermal atomic oxygen. Many of these cylinders are proposed to originate at defect sites. Images collected from both atomic force microscopy (AFM) and scanning tunnelling microscopy (STM) illustrate that the diameters of these cylinders increase linearly as a function of exposure. The overall distribution of pit diameters broadens with increasing exposure. In other words, several small cylinders are observed in every image, regardless of $O(^3P)$ fluence. With the larger exposure fluences ($> 10^{20}$ atoms cm^{-2}), however, giant, micron scale pit diameters are imaged. Therefore, it is suggested that the cylinders with the largest diameters are nucleated at or near the top sheet of the original HOPG surface. A large distribution of pit depths for cylinders of a specific diameter is also observed. This fact, in addition to the linearity of the overall erosion yield, suggests that the physical and chemical nature of the nucleation event has a marked impact on the overall morphology of the cylinders. The sites for these nucleation events may be point defects, long-range imperfections, or pristine areas of the HOPG surface. All of these avenues must be considered in order to fully describe the overall reactivity of the interface.

2. EXPERIMENTAL DETAILS

These experiments were performed at two locations in order to take advantage of complementary facilities and capabilities at these research institutions. Highly-ordered pyrolytic graphite (HOPG) surfaces (SPI-Materials—ZYA Grade) were cleaned and then exposed to hyperthermal $O(^3P)$ atoms at Montana State University. AFM and STM imaging and the associated analyses were completed at The University of Chicago.

A pulsed beam containing ~ 5 eV $O(^3P)$ atoms and O_2 was directed at an HOPG surface (1 cm \times 1 cm). Before exposure, the HOPG sample was cleaved several times using Scotch tape to yield several large terraces that did not contain any defects. This was confirmed by atomically-resolved STM. The molecular beam source is based on the laser detonation apparatus originally developed by Physical Sciences, Inc. A piezoelectric pulsed valve was employed to inject a packet of O_2 gas (18 bars of pressure) into a water-cooled, gold-plated copper nozzle. The dimensions, detailed design of this experimental apparatus, and beam characterization methods have been described elsewhere [10–12]. The sample mount, whose temperature can be controlled from 298 to 573 K, was located 40 cm from the nozzle orifice. The sample temperature for all of the exposures reported herein is 373 K. The incident angle of the $O_2 + O$ beam on the samples was a few degrees ($< 5^\circ$)

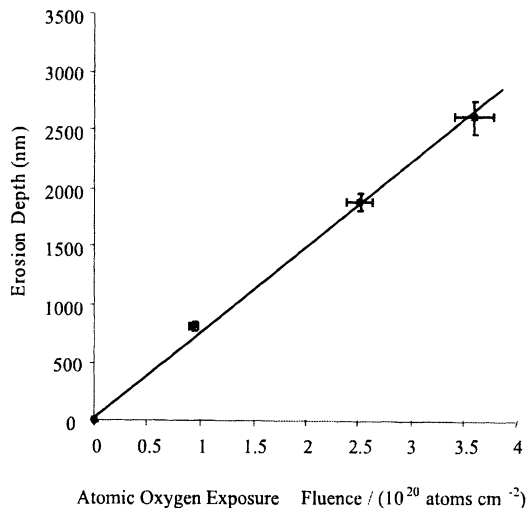


Figure 1. Overall erosion depth of HOPG plotted as a function of atomic oxygen exposure. The sample was exposed at 373 K. The depths were measured using profilometry.

from the surface normal. Samples were generally exposed for several hours at a rate of two pulses of $\text{O}(^3P)$ atoms per second. On average, each pulse contained 1.75×10^{15} O atoms (mean translational energy of ~ 5 eV) and lasted for < 100 ms. Therefore, the estimated atomic oxygen exposure rate at this distance was $\sim 3.5 \times 10^{15}$ atoms $\text{cm}^{-2} \text{s}^{-1}$. The fluence measurements were determined by using the erosion depth of a Kapton H standard and assuming an erosion yield for Kapton H of 3.00×10^{24} cm^3 O atom $^{-1}$. The beam diameter was large enough to encompass the entire sample mount.

An etched mesh of stainless steel was placed over the samples during the exposures in order to facilitate measurements of step height with a profilometer and thereby determine erosion yield. The surface morphology of the reacted HOPG was imaged using a Topometrix Discoverer AFM/STM system. Due to the roughness of the exposed samples, AFM rather than STM was employed most frequently in the analyses. All of the images contained in this paper were taken at 500 dpi resolution and have been levelled using a three-point scheme. Line scans, surface roughness, and other image analyses were accomplished using Topometrix software. All imaging of the HOPG surfaces was conducted at room temperature.

3. RESULTS AND DISCUSSION

The erosion rate of HOPG upon exposure to hyperthermal atomic $\text{O}(^3P)$, as measured by profilometry, has been determined to increase as a function of sample temperature at

a constant fluence [9]. At a sample temperature of 300 K, ~ 1 C atom is removed for every 22 incident oxygen atoms (fluence = 1.8×10^{20} atoms cm^{-2}) [9]. When the sample temperature is elevated to 493 K, ~ 1 C atom is etched for every eight incident O atoms (fluence = 2.0×10^{20} atoms cm^{-2}) [9]. This observation has been directly correlated with an elevated surface roughness at the higher sample exposure temperature and therefore an increased number of available prism plane sites on the graphite surface for reactivity [9]. Due to their inherent electronic structure, the prism sites have been shown to be far more reactive to O_2 and atomic oxygen than the basal plane [13].

Figure 1 illustrates the erosion yield of HOPG upon exposure to the hyperthermal O-atom beam as a function of Kapton-equivalent fluence at a constant temperature of 373 K. The rate of reaction appears to be linear ($R^2 = 0.993$) for the exposure range of 9.4×10^{19} to 3.6×10^{20} atoms cm^{-2} . An exposure of 5.0×10^{18} atoms cm^{-2} was also performed, but the etching depth was not sufficient to measure with profilometry and is therefore not included on this plot. For 373 K, the measured erosion yields correlate to ~ 1 C atom being etched for every 16 incident oxygen atoms.

Numerous cylindrical pits are observed in the eroded areas, regardless of hyperthermal atomic oxygen fluence. Images of the progression from a pristine, atomically perfect, HOPG surface to an eroded surface containing several cylindrical pits are portrayed in figure 2. Figure 2(a) represents an STM image of a freshly cleaved HOPG surface ($10 \text{ nm} \times 10 \text{ nm}$) where the original basal plane of graphite is clearly resolved. Figures 2(b) ($2 \mu\text{m} \times 2 \mu\text{m}$) and 2(c) ($4 \mu\text{m} \times 4 \mu\text{m}$) are AFM images of an eroded HOPG surface after exposure ($T_{\text{sample}} = 373 \text{ K}$) to 1.5×10^{19} and 9.4×10^{19} O atoms cm^{-2} , respectively.

Most of the pit features are cylindrical in nature. The shape is similar to that observed for the O_2 chemistry of HOPG where point defects (missing C atoms) are believed to be the nucleation sites [3]. Theoretically, oxygen is proposed to remove one C atom adjacent to the defect, only to open more reactive sites (C atoms in the prism plane) [14]. This O_2 reactivity leads to cylinders whose diameter depends upon exposure. The depths of the cylinders span from monolayer to multilayer, are thought to depend upon the depth of the defect, and the rest of the graphite basal plane remains pristine.

Despite the striking similarities between the shapes of the etch pits, it must be mentioned that it has been demonstrated that HOPG, both the basal plane and defect sites, are virtually unreactive to O_2 at sample temperatures below 775 K [5]. The reactivity of HOPG with hyperthermal atomic oxygen has been previously demonstrated even at room temperature [9]. After exposure to 2.5×10^{20} atoms cm^{-2} , $> 2 \mu\text{m}$ of the original material is completely eroded at $T_{\text{sample}} = 373 \text{ K}$; therefore, it appears that the basal plane C atoms are also reactive, not just defect sites. The eroded HOPG surface that contains embedded cylindrical pits is *not* atomically flat, unlike the O_2 /HOPG combustion chemistry just described. The mean RMS surface roughness for a $7 \mu\text{m} \times 7 \mu\text{m}$ cross-section is 8–16 nm. It is also interesting to note that the bases of the deep etch pits are not atomically flat either. This will be the topic of a future publication [15].

The relationship between the diameter of the *largest* cylindrical pits (top 10%) and the fluence of hyperthermal oxygen atoms is illustrated in figure 3. The pit diameter increases linearly ($R^2 = 0.985$) with higher exposures. (The average overall diameter of the cylinders

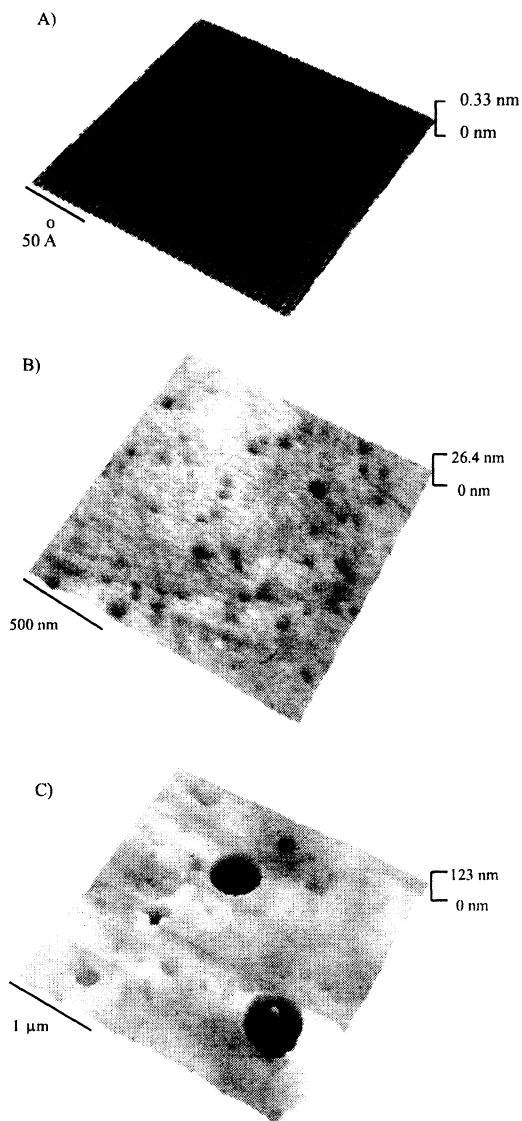


Figure 2. (a) STM image ($10 \text{ nm} \times 10 \text{ nm}$) of ZYA-Grade HOPG. The atomic lattice of graphite is clearly shown. (b) AFM image ($2 \mu\text{m} \times 2 \mu\text{m}$) of HOPG after exposure to 1.5×10^{19} O atoms cm^{-2} . (c) AFM image ($4 \mu\text{m} \times 4 \mu\text{m}$) of HOPG after exposure to 9.4×10^{19} O atoms cm^{-2} . The experiments were conducted at a sample temperature of 373 K.

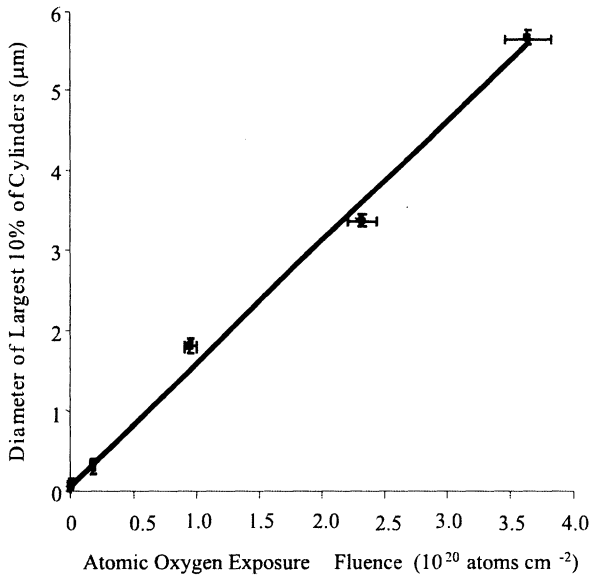


Figure 3. Mean diameter of the largest cylindrical pits as a function of atomic oxygen exposure. The samples were reacted at a temperature of 373 K. The diameters were measured by AFM. The plot represents the largest 10% of etch pits for each experiment.

rises linearly with fluence as well, but this observation is not as pertinent to this discussion.) Numerous small pits [~ 12 for every $1 \mu\text{m}^2$ for the experiments represented by figures 2(b) and 2(c)], a few nanometers in diameter, are observed in all of the erosion experiments. For the largest cylinders, the difference in pit diameter with respect to fluence is quite profound, ~ 125 nm in figure 2(b) and $\sim 1 \mu\text{m}$ in figure 2(c), respectively. Cylinders with diameters spanning the range from several hundred nanometers to microns often have one or more smaller pits embedded inside them. Pit-merging events, where two cylinders (of various sizes) have been eroded sufficiently enough in the prism plane direction to come together and make one feature, have also been imaged. Merging events have been observed most commonly for the smaller cylinders.

The diameter of the cylinders with respect to hyperthermal O-atom exposure provides insight into the nature of the erosion of graphite at a fundamental level ($T_{\text{sample}} = 300\text{--}375$ K). As the diameters of the widest 10% of the etch pits increases linearly with increased O atom fluence, the nucleation events of those cylinders must have occurred at or near the topmost graphite layer, otherwise the same distribution of pit diameters would be observed regardless of exposure. Therefore, the chemical impact of the nucleation site, a cylindrical etch pit, may still persist after several microns of the material have been eroded by hyperthermal atomic oxygen.

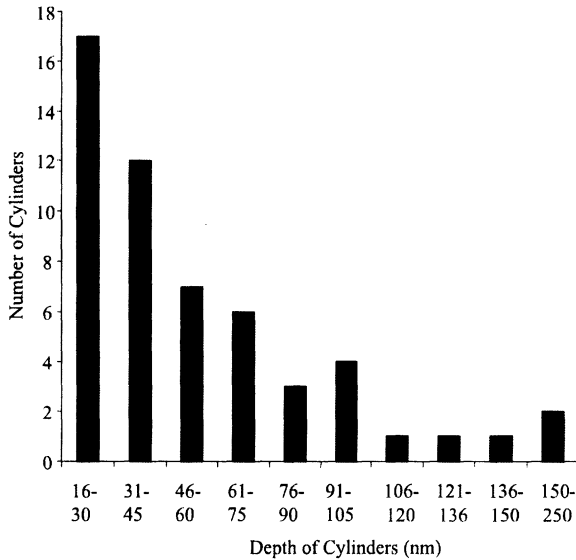


Figure 4. Histogram of cylinder depths at a diameter of $2.0 \mu\text{m} \pm 100 \text{ nm}$. The atomic oxygen fluence was $9.4 \times 10^{19} \text{ O atoms cm}^{-2}$ and the sample temperature was 373 K during exposure. The mean depth for the 55 cylinders is 56 nm. The cylinder diameters and depths were measured by AFM.

This impact further manifests itself in the depth profile of these large cylindrical pits. Figure 4 illustrates a histogram that describes the measured depths of 55 cylinders with diameters intentionally selected to be $2.0 \mu\text{m} (\pm 100 \text{ nm})$. The mean and median depths are 56 nm and 36 nm respectively. The largest number of pits (17) have been found in the 16–30 nm category. A constant diameter has been chosen in order to measure the variance of cylinder depth for etch pits that originate at a similar point in time.

The depth histogram may be quite surprising given the linear pit diameter growth (fig. 3) and erosion yield (fig. 1) as a function of atomic oxygen exposure. If these trends are indeed linear, one would expect the diameter and depth to grow according to the respective rate constants, k_{prism} and k_{basal} . Therefore, it is proposed that these large, very deep, cylinders often nucleate at long-range defects, such as line defects or domain boundaries. The defects have more edge atoms (k_{prism}) exposed and are reacted by hyperthermal atomic oxygen at a higher rate at the beginning of the erosion process than the basal plane atoms. In other words, the C atoms that comprise the defect site are etched in both dimensions, downward into the material and outward in the prism plane direction, at the faster k_{prism} rate. This process provides the head start necessary to yield deep etch pits, a depth that clearly must be influenced by the chemical and physical nature of the original defect site. Therefore, defects that extend deep into the material, hundreds and possibly thousands of atomic layers, are expected to lead to the deepest cylinders

in the eroded areas. However, this analysis does not eliminate the possibility that rare catalytic events can occur at perfect and imperfect regions of the HOPG surface that result in cylindrical pits.

This information can also be used to provide insight into the origin of the numerous small pits that are imaged at every exposure snapshot. The observed deep pits (> 15 nm) with small diameters nucleate at regions of the surface uncovered during the erosion process. Shallow cylinders (< 15 nm) are imaged with small diameters, often on the order of a few nanometers. These pits arise from either nucleation occurring at defects or reactions occurring at pristine regions of a fresh graphite sheet uncovered during the erosion process. It appears that these pits eventually merge with other cylinders or additional features in the eroded areas before their diameters approach the micron scale. It must be noted that no pits have been observed with diameters of $2 \mu\text{m}$ and a depth of less than 15 nm (fig. 4). This is not surprising given that the RMS roughness of the eroded areas is similar to the depths of these shallow cylinders.

4. CONCLUSIONS

This paper discusses the erosion of HOPG upon exposure to hyperthermal atomic oxygen, highlighting the role of long-range defects in materials chemistry and degradation. HOPG has been observed to erode at a rate of ~ 1 C atom for every 16 incident $\text{O}(^3P)$ atoms when the sample temperature is 373 K during exposure. This rate appears to be linear as a function of fluence. This erosion rate encompasses reactivity arising concurrently from both atomically perfect regions of the interface as well as those that contain defect sites.

Nanoscale to microscale cylinders have been imaged using both AFM and STM. The mean diameter of the etch pits increases linearly with 5 eV $\text{O}(^3P)$ fluence. Specifically, the largest cylinders (diameter > 500 nm) are only observed after the longest exposures while numerous small pits are imaged after every experiment, regardless of exposure duration. Therefore, cylinders with the largest diameters nucleate at or near the top of the material.

Etch pits of the same diameter have a wide variety of depths. For example, cylinders with a diameter of $2 \mu\text{m}$ are observed to have depths ranging 16–238 nm. Given the linearity of the overall erosion yield and pit diameter as a function of atomic oxygen exposure, the variety of depths may be explained by the nature of the nucleation event. That is, the long-range defects that exist at or near the surface as well as those which are buried deep within the HOPG material play a critical role in the erosion and morphological evolution of the surface. In addition, rare catalytic events that can occur at perfect and imperfect regions of the surface may also contribute to the creation of cylindrical pits. The atomic-level mechanisms responsible for cylindrical pit formation and the overall erosion of HOPG are currently being investigated by theory and experiment.

Acknowledgements. These experiments were primarily supported by the AFOSR sponsored MURI Center for Materials Chemistry in the Space Environment. Supplemental support from The University of Chicago Argonne National Laboratory Consortium for Nanoscience Research and the National Science Foundation-Materials Research Science and Engineering Center at the University of Chicago are also

gratefully acknowledged. Jalice Manso is thanked for her assistance in the profilometry measurements and the atomic oxygen exposures. Amadou Cisse and Devon Pennington are thanked for their contributions in sample imaging.

NOTE

1. Authors to whom correspondence should be addressed: e-mail: s-sibener@uchicago.edu and tminton@montana.edu

REFERENCES

- [1] Banks B A, de Groh K K, Rutledge S L and DiFillipo F J 1996 *Prediction of In-Space Durability of Protected Polymers Based on Ground Laboratory Thermal Energy Atomic Oxygen*, (Washington, DC: NASA)
- [2] Murad E 1996 *J. Spacecraft Rockets* **33** 131
- [3] Charlier M.-C. and Charlier A 1987 *Chemistry and Physics of Carbon* P. A. Throver (ed) (New York: Marcel Dekker) Vol. 20
- [4] Olander D R, Siekhous W, Jones R and Schwarz J A 1972 *J. Chem. Phys.* **57** 408
- [5] Stevens F, Kolodny L A and Beebe T P 1998 *J. Phys. Chem. B* **102** 10799
- [6] Zhu Y, McBride J D, Hansen T A and Beebe, T P 2001 *J. Phys. Chem. B* **105** 2010
- [7] McBride J D, Tessell B V, Jachmann R C and Beebe T P 2001 *J. Phys. Chem. B* **105** 3972
- [8] Ngo T, Snyder E J, Tong W M, Williams R S and Anderson M S 1994 *Surf. Sci.* **314** L817
- [9] Nicholson K T, Minton T K and Sibener S J 2003 *Prog. Org. Coat.* **47** 443
- [10] Minton T K and Garton D J 2001 *Advanced Series in Physical Chemistry: Chemical Dynamics in Extreme Environments* Dressler R A (ed) (Singapore: World Scientific) p 420
- [11] Zhang J, Garton D J and Minton T K 2002 *J. Chem. Phys.* **117** 6239
- [12] Brunsvold A L, Minton T K, Gouzman I, Grossman E and Gonzalez R 2003 *High Perform. Polymers* this issue.
- [13] Olander D R, Jones R H, Schwarz J A and Siekhaus W J 1972 *J. Chem. Phys.* **57** 421
- [14] Lee S M, Lee Y H, Hwang Y G, Hahn, J R and Kang H 1999 *Phys. Rev. Lett.* **82** 217
- [15] Nicholson K T, Minton T K and Sibener S J to be submitted.